

# Facile Removal of Pesticides from Aqueous Solutions Using Magnetic Nanocomposites

## I. Synthesis and characterization of the adsorbent material

IRINA FIERASCU<sup>1</sup>, RALUCA SOMOGHI<sup>1</sup>, CRISTIAN ANDI NICOLAE<sup>1</sup>, NICOLAE STANICA<sup>2</sup>, RADU CLAUDIU FIERASCU<sup>1\*</sup>

<sup>1</sup>National Institute for Research & Development in Chemistry and Petrochemistry - ICECHIM Bucharest, 202 Splaiul Independentei, 060021, Bucharest, Romania

<sup>2</sup> Ilie Murgulescu Institute of Physical Chemistry, 202 Splaiul Independentei, 060021, Bucharest, Romania

*An inorganic/organic magnetic nanocomposite was synthesized and analytically characterized using X-ray fluorescence, X-ray diffraction, transmission electron microscopy and thermal analysis. The evaluation of the magnetic properties revealed that both the magnetite and the magnetite/chitosan nanocomposite are superparamagnetic with a paramagnetic component, having the saturation magnetization values of 48.04 emu/g, and 41.3 emu/g, respectively. The synthesized material is intended for the adsorption of two known commercial-available pesticides (active ingredients deltamethrin and thiamethoxam, respectively) from aqueous solutions.*

**Keywords:** magnetic nanocomposites, characterization, XRD, thermal analysis, magnetic properties

The existence of clean water sources is a major concern worldwide. Due to the diversity of industrial and agricultural activities anything can come across in the polluted aqueous effluents like: pesticides, personal care products, heavy metals, pharmaceuticals, dyes, etc. Agriculture is the largest user of freshwater resources, but also the principal polluter. The increasing growth demand for agriculture products led to a proportional growth in the use of synthesized pesticides, having beneficial aspects on one hand, and produce loss on another hand, agriculture being cause and victim of water pollution [1].

A significant part of pollutants escapes the current treatment methods and reach surface and ground waters; in order to enhance the processes to remove pollutants from waters nanotechnologies can be harnessed to solve critical development problems, including wastewater pollution. Several published studies describe different methods of degradation or removal pesticides from different classes, such as photocatalysis [2], ozonation [3], adsorption [4-6] or biodegradation [7].

The adsorption studies were mainly focused on the development and application of new adsorbents, the most promising materials being the activated carbon [8] (used for the removal of a series of herbicides), carbon nanotubes [9] (used for the adsorption of fenuron pesticide) or natural polymers, such as cyclodextrin [10] or chitosan [11]. Another approach for the development of the next-generation adsorbents is represented by the core-shell nanostructures, having as main advantage the possibility to be applied in industrial application, as well as their facile removal, after their utilization, by applying an external magnetic field. The approach was used by several authors for developing core-shell structures applied in adsorption studies of different types of pollutants (Fe<sub>3</sub>O<sub>4</sub>/SiO<sub>2</sub> for the adsorption of dyes [12] or insecticides [13] or  $\alpha$ -Fe/EDTA for the adsorption of metallic ions [14]).

The present work describes the synthesis and characterization of magnetic core-shell nanostructures designed for the removal of pesticides from aqueous solutions.

### Experimental part

#### Synthesis of the adsorbent materials

The inorganic/organic magnetic composites used as adsorbents were building a chitosan shell over a magnetite core. The magnetite was obtained using a co-precipitation method from chloride precursors, after a recipe previously described [15]. The adsorbent magnetic composites were obtained by grafting a layer of chitosan (CS) over the magnetite. A CS solution, obtained by dissolving CS (Sigma Aldrich, USA, deacetylation degree 86%) in 1% (w/v) acetic acid solution was dropped over a CTAB (Fisher Scientific, USA) solution containing the magnetite. After a reaction time of four hours (under vigorous stirring), the obtained magnetic materials were separated using an external magnetic field, washed with distilled water and ethanol and dried at 45°C for 24 hours. The final composites were obtained by placing the dried materials in formaldehyde vapours for 48 hours (thus obtaining the crosslinking of the chitosan) [16]. Similar composites were also described by other authors as efficient adsorbents for Cr(VI) [17].

#### Analytical methods

Synthesis of the adsorbent materials was confirmed using X-ray fluorescence (XRF), X-ray diffraction (XRD), transmission electron microscopy (TEM) and thermal analysis. XRF spectra of the analysed samples were obtained using a PW4025 MiniPal2 PANalytical EDXRF Spectrometer: analysis gas -helium, analysis time -300 sec., X-ray tube voltage - 20 kV. XRD diffractograms were obtained using a Rigaku SmartLab diffractometer using Cu<sub>K $\alpha$</sub>  radiation ( $\lambda = 1.54059 \text{ \AA}$ ) operating at 40 kV and 200 mA, in parallel beam configuration (2 $\theta$ / $\theta$ ), between 15 – 90 degrees (2 $\theta$ ). The diffractograms were analysed using PDXL Program (database provided by ICDD). The crystallite size was estimated from the XRD data using the Scherrer equation [18]:

$$L = \frac{K\lambda}{\beta \cos\theta} \quad (1)$$

where: L - crystallite size, K - Scherrer constant,  $\lambda$  -X-ray wavelength,  $\beta$  -Full width at half-maximum of the peak,  $\theta$  -diffraction angle.

\* email: radu\_claudiu\_fierascu@yahoo.com

The transmission electron microscopy (TEM) images were obtained with a HRTEM - High Resolution Transmission Electron Microscope type TECNAI F30 G2STWIN at 300 kV acceleration voltage, having a resolution of 1 Å. The thermal behavior of the samples was determined using a TGA Q5000 (TA) instrument, heating rate of 10°C/min., between 24 and 700°C, purge gas nitrogen (99.999%), 50 ml/min.

As the magnetic character of the adsorbent is of great importance for the easy removal from aqueous solutions, magnetization versus magnetic field strength were performed on a Lake Shore's fully integrated Vibrating Sample Magnetometer system 7404 at room temperature, using nitrogen gas, in variable magnetic field [0 - 21,700] Oe, resolution of magnetization:  $0.1 \times 10^{-6}$  emu; step control of applied magnetic field: 70 mOe; moment stability:  $\geq \pm 0.05\%$  of full scale/day for fixed coil, constant field and temperature; resolution of magnetic field intensity: 3 ppm resolution; standard procedures for periodical calibration based on NIST standards (SRM 772a, SRM 762, SRM 2853) [15].

## Results and discussions

The first step in confirming the synthesis of the adsorbents was represented by the XRF analyses. Figure 1 presents the XRF spectra of the ferrite sample and the core/shell adsorbent.

The decrease observed in the specific lines of iron represents a decrease in the relative concentration of iron, suggesting the apparition of an organic shell (that cannot be determined *via* XRF). In the same time, the removal of the CTAB was confirmed by the absence of Br-specific lines ( $K\alpha$  -11.907 and  $L\alpha$  -1.480 keV, indicated by arrows on figure 1).

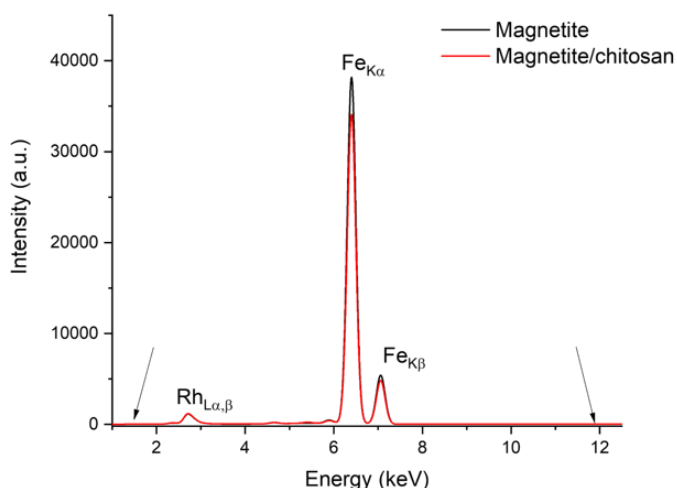


Fig. 1 XRF spectra of the magnetite precursor and the core-shell nanocomposite

X-ray diffraction analyses (figure 2) confirmed the structure of the magnetite precursor, by comparison with the entries in the ICDD database (PDF card no. 01-088-0866). The addition of a chitosan layer is confirmed by the

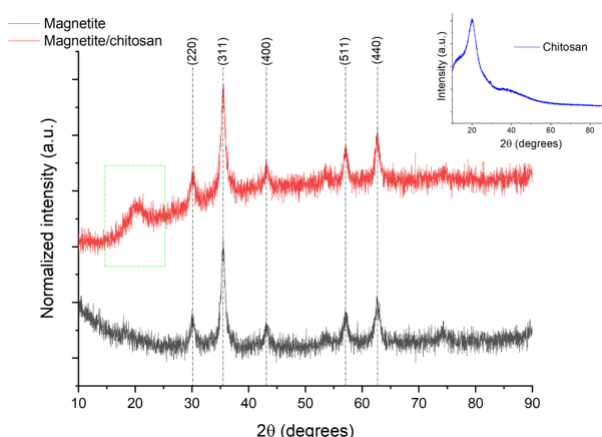


Fig. 2 XRD diffractograms of the samples: magnetite, magnetite/chitosan nanocomposite; inset -chitosan diffractogram

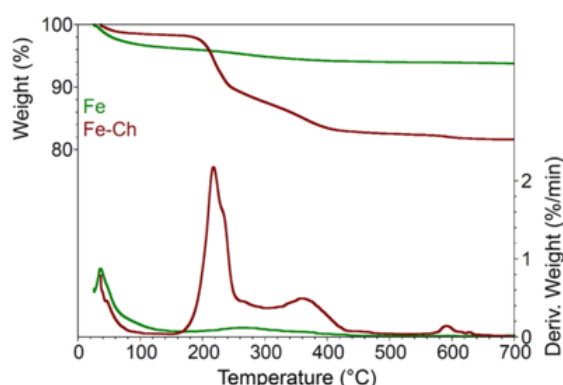


Fig. 3 TG and DTG curves of the magnetic precursor and organic/inorganic composite

apparition of the specific amorphous halo of chitosan around 20 degrees ( $2\theta$ ), indicated in green on figure 2 [19].

The size of the magnetite particles determined using the equation (1) [15], from the values of the diffraction peak corresponding to the (311) plane, was found to be approx. 10.07 nm.

The thermal properties of the magnetic precursor and of the final composite are presented in Figure 3 and Table 1.

For the magnetite sample, the thermal analysis reveals a mass loss up to 150°C of 3.78% (Table 1); the loss is attributed to the evaporation of water and OH groups from the surface of the sample. The weight loss recorded in the two other temperature ranges are in good concordance with literature data and the results previously obtained by our group on magnetite samples [15, 20].

The final composites show a much smaller weight loss in the first region (approx. 45% of the loss recorded for magnetite) which can be assigned to the formaldehyde treatment [16]. The two major weight losses recorded up to 500 °C are specific to the decomposition of chitosan crosslinked with formaldehyde and, respectively, chitosan residues, as observed by our group, as well as by other authors [16, 21]. The final residue found for the composite materials suggest a chitosan content of approx. 12%.

Sample	TGA/DTA( $\Delta G/T_{max}(\%wt/^\circ C)$ )			
	RT-150°C	150-500°C	500-700°C	Residue (%)
Magnetite	3.78/-	2.24/259.9	0.23/588.3	93.65
Magnetite/chitosan composite	1.71/-	10.74/217.2 5.05/358.7	0.69/591.1	81.82

**Table 1**  
WEIGHT LOSS RECORDED BY  
THERMAL ANALYSES

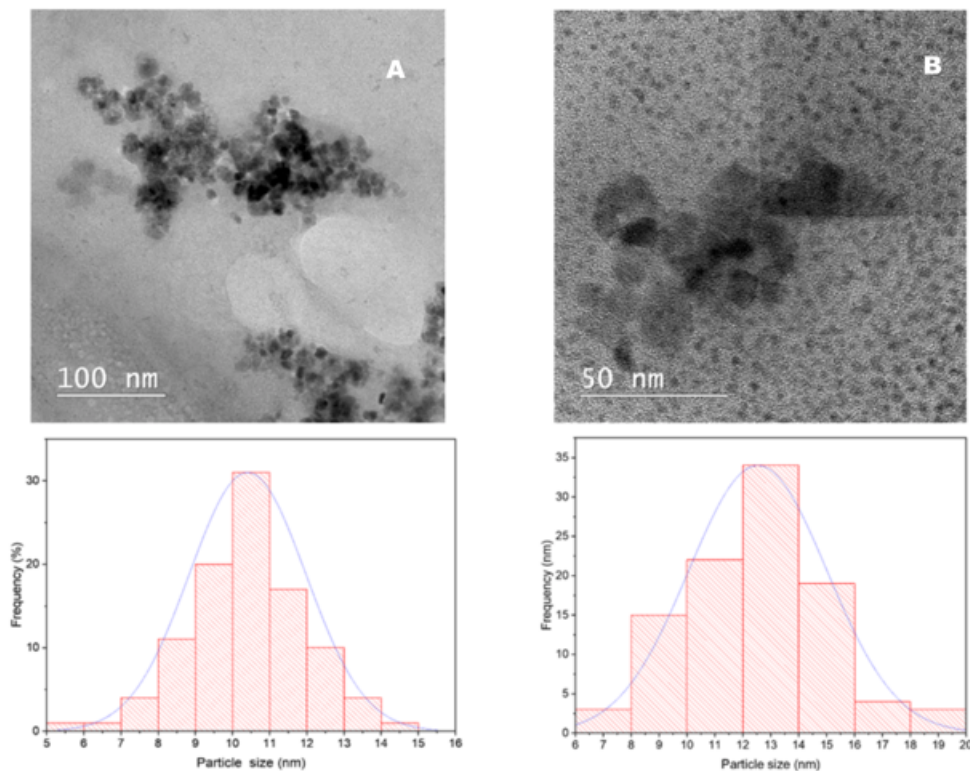


Fig. 4 TEM images and size distribution of the analyzed materials

Sample	Magnetic properties			
	$M_s$ (emu/g)	$\mu/k$ (K/Oe)	$\chi_s$ ( $\times 10^{-6} \text{ cm}^3/\text{g}$ )	$\chi^2$ ( $\times 10^{-4}$ )
Magnetite	48.0	1.2	983.9	4.3
Magnetite/chitosan composite	41.3	1.2	735	4.0

**Table 2**  
MAGNETIC PROPERTIES OF THE ANALYZED SAMPLES

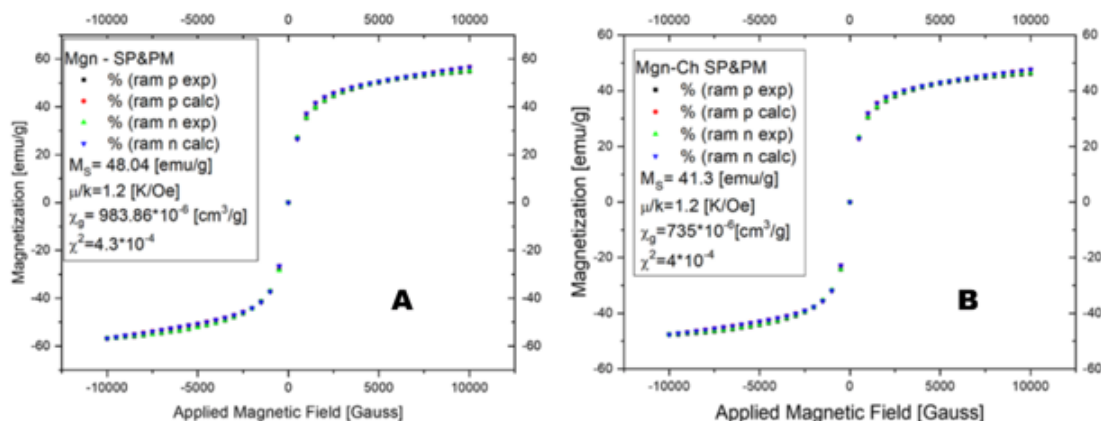


Fig. 5 Experimental and calculated magnetic data for magnetization loop, for the studied samples: left - magnetite, right - magnetite/chitosan composite; *ram P* - part of hysteresis loop for descending magnetic field; *ram N* - part of hysteresis loop for ascending magnetic field

The analysis of the TEM images (figure 4) shows spherical magnetite nanoparticles, with average size of approx. 10 nm, in good agreement with the XRD determinations; another important observation that can be made is that the polymer coating prevented the aggregation of the particles. The analysis of the composites reveals a slight increase of the particle dimensions, due to the polymer coating.

The magnetic properties were determined for both the magnetite and the magnetite/chitosan composite. By analyzing the magnetization curves (presented in figure 5) and the obtained values (Table 2), there can be observed that both analyzed samples are superparamagnetic with a paramagnetic component. The superparamagnetic

properties of the analyzed samples can be also correlated with the value of the crystallite size.

From the presented data in Table 2 it can be observed a slight decrease of the saturation magnetization value ( $M_s$ ) obtained for the composite (from 48.04 emu/g to 41.3 emu/g), both much higher compared with our previous results [15]. The relative preservation of the magnetic properties makes the composites available for magnetic separations in environmental applications.

## Conclusions

A magnetic nanocomposite was obtained, using magnetite as the magnetic core and crosslinked chitosan as the external, adsorbent material. The analytical results confirmed the synthesis of the nanocomposite, while the

evaluation of the magnetic properties suggests the superparamagnetic with paramagnetic component nature of both the magnetite precursor and the final nanocomposite.

*Acknowledgements: This work was supported by a grant of the Romanian National Authority for Scientific Research and Innovation, CNCS/CCCDI – UEFISCDI, project number PNIII-P2-2.1-PTE-2016-0063, within PNCDI III and by Romanian Ministry of Research and Innovation - MCI through INCDCP-ICECHIM 2019-2022 Core Program, Project PN 19.23.03.01. The authors would like to thank prof. Dan Donescu for the critical reading of the manuscript and the valuable advices.*

## References

1. EVANS, A.E.V., MATEO-SAGASTA, J., QADIR, M., BOELEEE, E., IPPOLITO, A., *Curr. Opin. Env. Sust.*, **36**, 2019, p. 20.
2. BERBERIDOU, C., KITSIOU, V., LAMBROPOULOU, D.A., ANTONIADIS, A., NTONOU, E., ZALIDIS, G.C., POULIOS, I., *J. Environ. Manage.*, **195**, 2017, p. 133.
3. ZHAO, Q., GE, Y., ZUO, P., SHI, D., JIA, S., *Chemosphere*, **146**, 2016, p. 105.
4. MANSOURIIEH, N., SOHRABI, M.R., KHOSRAVI, M., *Int. J. Environ. Sci. Technol.*, **13**, 2016, p. 1393.
5. NEAGU, M., POPOVICI, D.R., DUSESCU, C.M., CALIN, C., *Rev. Chim. (Bucharest)*, **68**, no. 1, 2017, p. 139.
6. LARION, M., MURESAN, E.I., RADU, C.D., SANDU, I., CEREMPEI, A., CIMPOESU, N., *Rev. Chim. (Bucharest)*, **69**, no. 1, 2018, p. 228.
7. POURBABAEI, A.A., SOLEYMANI, S., FARAHBAKHS, M., TORABI, E., *Int. J. Environ. Sci. Technol.*, **15**, 2018, p. 1073.
8. DERYLO-MARCZEWSKA, A., BLACHNIO, M., MARCZEWSKI, A.W., SECZKOWSKA, M., TARASIUK, B., *Chemosphere*, **214**, 2019, p. 349.
9. ALI, I., ALHARBI, O.M.L., ALOTHMAN, Z.A., AL-MOHAIMEED, A.M., ALWARTHAN, A., *Environ. Res.*, **170**, 2019, p. 389.
10. LIU, H., CAI, X., WANG, Y., CHEN, J., *Water Res.*, **45**, No. 11, 2011, p. 3499.
11. SHANKAR, A., KONGOT, M., SAINI, V.K., KUMAR, A., *Arab. J. Chem.*, 2018, DOI: 10.1016/j.arabjc.2018.01.016.
12. GHORBANI, F., KAMARI, S., *Environ. Technol. Innov.*, **14**, 2019, 100333.
13. FARMANY, A., MORTAZAVI, S.S., MAHDAVI, H., *J. Magn. Mater.*, **416**, p. 75.
14. AZZAM, A.M., SHENASHEN, M.A., SELIM, M.M., YAMAGUCHI, H., EL-SEWIFY, I.M., KAWADA, S., ALHAMID, A.A., EL-SAFITY, S.A., *J. Phys. Chem. Solids*, **109**, 2017, p. 78.
15. DONESCU, D., FIERASCU, R.C., GHIUREA, M., MANAILA-MAXIMEAN, D., NICOLAE, C.A., SOMOGHI, R., SPATARU, C.I., STANICA, N., RADITOIU, V., VASILE, E., *Appl. Surf. Sci.* **414**, 2017, p. 8.
16. FIERASCU, R.C., DINU-PIRVU, C.E., FIERASCU, I., ARMURE, V., STANICA, N., NICOLAE, C.A., SOMOGHI, R., TRICA, B., ANUA, V., *Farmacia*, **66**, 2018, p. 316.
17. ZHANG, B., WU, Y., FAN, Y., *J. Inorg. Organometall. Polym. Mater.*, **29**, 2019, p. 290.
18. NWANKWO, U., BUCHER, R., EKWEALOR, A.B.C., KHAMLICH, S., MAAZA, M., EZEMA, F.I., *Vacuum*, **161**, 2019, p. 49.
19. MENDES, J.F., PASCHOALIN, R.T., CARMONA, V.B., SENA NETO, A.S., MARQUES, A.C.P., MARCONCINI, J.M., MATTOSO, L.H.C., MEDEIROS, E.S., OLIVEIRA, J.E., *Carbohydr. Polym.*, **137**, 2016, p. 452.
20. THOMAS, G., DEMOISSON, F., BOUDON, J., MILLOT, N., *Dalton Trans.*, **45**, 2016, 10821.
21. KYZAS, G.Z., DELIYANNI, E.A., *Molecules*, **18**, 2013, 6193.

---

Manuscript received: 19.03.2019